Evidence for an Active Role of $IF3_{mt}$ in the Initiation of Translation in Mammalian Mitochondria[†]

Brooke E. Christian and Linda L. Spremulli*

Department of Chemistry, University of North Carolina, Chapel Hill, North Carolina 27599-3290

Received December 23, 2008; Revised Manuscript Received February 18, 2009

ABSTRACT: Mitochondrial translational initiation factor 3 ($IF3_{mt}$) is a 29 kDa protein that has N- and C-terminal domains, homologous to prokaryotic IF3, connected by a linker region. The homology domains are preceded and followed by short extensions. No information is currently available on the specific residues in $IF3_{mt}$ important for its activity. On the basis of homology models of $IF3_{mt}$, mutations were designed in the N-terminal, C-terminal, and linker domains to identify the functionally important regions. Mutation of residues 170−171, and 175 in the C-terminal domain to alanine resulted in a nearly complete loss of activity in initiation complex formation and in the dissociation of mitochondrial 55S ribosomes. However, these mutated proteins bind to the small (28S) subunit of the mammalian mitochondrial ribosome with K_d values similar to that of the wild-type factor. These mutations appear to lead to a factor defective in the ability to displace the large (39S) subunit of the ribosome from the 55S monosomes in an active process. Other mutations in the N-terminal domain, the linker region, and the C-terminal domain had little or no effect on the ability of $IF3_{mt}$ to promote initiation complex formation on mitochondrial 55S ribosomes. Mutation of residues 247 and 248 in the C-terminal extension abolished the ability of $IF3_{mt}$ to reduce the level of binding of fMet-tRNA to the ribosome in the absence of mRNA. Our results suggest that $IF3_{mt}$ plays an active role in initiation of translation.

Over the past several years, interest in understanding mammalian mitochondria has grown as the involvement of these organelles in a variety of diseases has become more apparent. In particular, dysfunctions in mitochondria and mutations in mitochondrial DNA have been linked to genetic diseases, Alzheimer's disease, Parkinson's disease, and other age-related neurodegenerative diseases (*1*). Before the relationship between mitochondria and disease states can be fully understood, a number of fundamental questions about mitochondrial processes, including mitochondrial gene expression, must be answered.

Mammalian mitochondria contain ~16 kb pairs of DNA (*2*). This genetic information encodes two rRNAs, 22 tRNAs, and 13 proteins. The DNA is circular and continuous; it lacks significant noncoding regions. All of the proteins encoded in this genome are hydrophobic membrane proteins that are subunits of either the oligomeric electron transfer complexes or the ATP synthase required for the generation of energy by the cell (*2*).

Translation of the mRNAs encoded by mitochondrial DNA requires the presence of a protein biosynthetic system that is distinct from that of the cell cytoplasm. Mitochondrial ribosomes are 55S particles that have approximately half the rRNA content and twice the protein content of bacterial ribosomes (*3*). Mitochondrial ribosomal subunits have sedimentation coefficients of 28S and 39S, while bacterial ribosomal subunits have sedimentation coefficients of 30S and 50S and form 70S monosomes.

Translation initiation factors have similarities in the bacterial and mitochondrial systems, but several key differences are apparent. Three essential translation initiation factors have been identified in *Escherichia coli*, while only two have been identified in the mitochondrial system. In *E. coli*, IF2[1] promotes the binding of fMet-tRNA to the P-site of the 30S ribosomal subunit and promotes the joining of the 30S and 50S ribosomal subunits (*4*). Mitochondrial IF2 ($IF2_{mt}$) appears to have the same fundamental activities found in its bacterial counterpart. IF1 in *E. coli* is an essential 71-amino acid protein whose exact function is unknown (*5*). No factor corresponding to IF1 has been identified in mitochondria. However, $IF2_{mt}$ has a 37-amino acid insertion that is believed to function in place of IF1 in translation (*6*).

In *E. coli*, IF3 is thought to have a number of roles. These include (1) dissociation of 70S monosomes into subunits by the preferential binding of IF3 to the small ribosomal subunit, (2) promotion of the formation of initiation complexes, (3) dissociation of initiation complexes with noncanonical start codons, (4) promotion of the shift of the mRNA start codon into the P-site of the small subunit, and (5) mediation of the codon−anticodon interactions of the initiator tRNA (*7*−*15*). Like *E. coli* IF3, $IF3_{mt}$ stimulates initiation complex formation in part by promoting the dissociation of 55S ribosomes, thereby providing free small subunits for initiation complex formation. $IF3_{mt}$ has an additional role not found in bacteria; it reduces the level of $IF2_{mt}$-mediated binding of fMet-tRNA

[†] This study was supported NIH Grant GM32734.

* To whom correspondence should be addressed. Phone: (919) 966-1567. Fax: (919) 843-1580. E-mail: Linda_Spremulli@unc.edu.

[1] Abbreviations: IF3, translation initiation factor 3; $IF3_{mt}$, human mitochondrial translation initiation factor 3; IF1, translation initiation factor 1; IF2, translation initiation factor 2; $IF2_{mt}$, bovine mitochondrial translation initiation factor 2.

10.1021/bi8023493 CCC: $40.75
Published on Web 02/24/2009

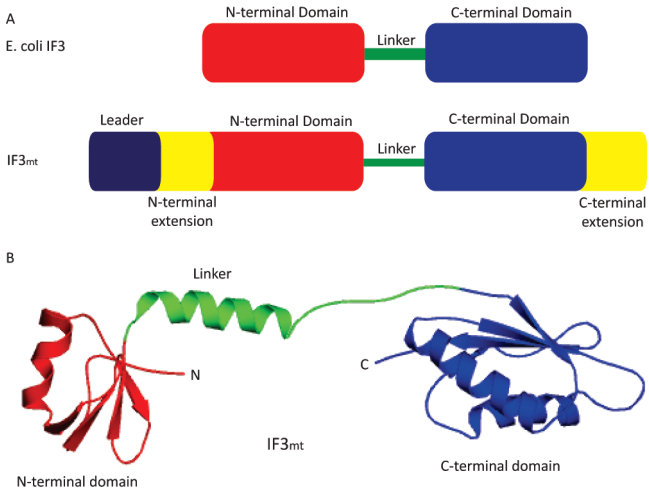

FIGURE 1: Domain organization and model of $IF3_{mt}$. (A) Schematic representation of *E. coli* IF3 and $IF3_{mt}$ showing the N- and C-terminal homology domains and the linker regions. $IF3_{mt}$ has additional N- and C-terminal extensions not present in the *E. coli* factor. The leader specifies mitochondrial import and is not present in the constructs used here. (B) Three-dimensional model of $IF3_{mt}$ prepared using Insight II. The N-terminal domain was modeled after the crystal structure of the N-terminal domain of *Bacillus stearothermophilus* IF3 [Protein Data Bank (PDB) entry 1TIF (*26*)], and the C-domain was modeled after the NMR structure of mouse $IF3_{mt}$ [PDB entry 2CRQ (unpublished)]. The N- and C-terminal extensions are not shown and are predicted to be disordered.

to 28S subunits in the absence of mRNA (*16*). This observation suggests that mRNA binding normally precedes fMet-tRNA binding in the mitochondrial system.

Following removal of the mitochondrial import signal, $IF3_{mt}$ is a 29 kDa protein composed of three regions that have homology to the bacterial factor: the N-terminal domain, the linker, and the C-terminal domain (Figure 1A). The N-terminal homology domain is preceded by an extension of 31 amino acids, and the C-terminal domain is followed by an extension of 33 amino acids. Most of the functions of *E. coli* IF3 and $IF3_{mt}$ tested in vitro have been localized to the C-terminal domain. Full-length $IF3_{mt}$ is thought to bind on the interface side of the small subunit close to the platform with a K_d of 30 nM (*17*). The isolated C-terminal domain of $IF3_{mt}$ also has a strong affinity for the 28S subunit and binds with a K_d of 95 nM (*17*). The isolated N-terminal domain of *E. coli* IF3 has no detectable binding to the 30S ribosomal subunit (*12*). This domain of IF3 is thought to increase the affinity of the intact IF3 protein for the 30S subunit by 2 orders of magnitude. In contrast, the isolated N-terminal domain of $IF3_{mt}$ binds to the 28S subunit with a K_d of 390 nM (*17*). The N- and C-terminal extensions of $IF3_{mt}$ are not required for binding of the protein to the small subunit, and removal of the extensions has almost no effect on the binding constant (*18*). However, the C-terminal extension, along with the linker, plays a role in preventing binding of fMet-tRNA to the 28S subunit in the absence of mRNA (*17*).

MATERIALS AND METHODS

Materials. Laboratory supplies and chemicals were purchased from Sigma-Aldrich or Fisher Scientific. A rabbit polyclonal primary antibody to the region of $IF3_{mt}$ homologous to the bacterial factors was prepared as previously described (*16*). Bovine mitochondrial ribosomes (55S), ribosomal subunits (28S and 39S), bovine $IF2_{mt}$, and yeast [^{35}S]fMet-tRNA were prepared as described previously (*19*−*21*).

Table 1: Summary of the Mutations Introduced into $IF3_{mt}$

mutation	location	residues mutated	residues changed to
$IF3_{mt}$:1	N-domain	KKTKK (66−70)	AATAA
$IF3_{mt}$:2	N-domain	TSTE (121−124)	AAAA
$IF3_{mt}$:3	linker	REMEK (143−147)	AAMAA
$IF3_{mt}$:4	C-domain	KKK (184−186)	AAA
$IF3_{mt}$:5	C-domain	HD (170 and 171)	AA
$IF3_{mt}$:6	C-domain	K (175)	A
$IF3_{mt}$:7	C-domain	K (194)	A
$IF3_{mt}$:8	C-domain	EE (207 and 208)	AA
$IF3_{mt}$:9	C-extension	EE (247 and 248)	AA
$IF3_{mt}$:10	C-extension	KE (252 and 253)	AA
$IF3_{mt}$:11	C-extension	DT (261 and 262)	AA
$IF3_{mt}$:12	C-extension	KD (265 and 266)	AA

Table 2: Forward Primers Used for Site-Directed Mutagenesis of $IF3_{mt}$[a]

$IF3_{mt}$:	Forward Primer
1a	GACAAAAGCGAATAAAACAGCTTTTAGTAACG
1b	AGACAGCAGCGAATAAAACAGCTTTTAGTAACG
1c	CACCCAGAATGAAGGAGCAAAGACAGCAGCG
1d	GAATGAAGGAGCAGCGACAGCAGCG
2	GGTTCAAAGGAACGCCGCCGCAGCACCTGCAGAGTAT
3a	CAGAGGCTGGCTGCGATGGAGAAGGCGAACCC
3b	GCTGCGATGGCTGCGGCGAACCC
4	GCAGTGGATTGCGGCAGCACACCTAGTCC
5	TCTTCAAATATTGGACAAGCTGCTTTGGACACAAAGACTAAACAG
6	GATTTGGACACAGCGACTAAACAGATTCAG
7	CCAGATTACCATAGCGAAAGGAAAAAATGTAGACG
8	GTCAGAAAATGAAATGGCGGCGATATTTCATC
9	GCTTTGAGCAAAAATGCGGCGAAGGCATATAAAG
10	GGAGAAGGCATATGCAGCAGAAACTCAAGAGACCC
11	GACCCAGGAAAGAGCCGCTTTGAACAAAGACC
12	GAGACACTTTGAACGCAGCCCATGGAAATGATAAGG

[a] Mutated nucleotides are highlighted in gray. The reverse primers used were the inverse complements of the forward primers in each case. To introduce the four-amino acid mutations into $IF3_{mt}$:1, four sequential mutations were required using primers 1a−1d sequentially. To introduce the four-amino acid mutations into $IF3_{mt}$:3, two sequential mutagenic reactions were carried out using primers 3a and 3b as indicated.

Preparation of Mutated Derivatives of $IF3_{mt}$. The sequence for $IF3_{mt}$ containing a six-histidine tag was previously cloned into the pET21c vector using NdeI and XhoI restriction sites (*22*). Twelve mutated derivatives, designated $IF3_{mt}$:1−12 (Table 1), were prepared by site-directed mutagenesis using the primers listed in Table 2 and the QuikChange site-directed mutagenesis protocol (Stratagene). All mutations were verified by DNA sequencing. The mutated plasmids were transformed into *E. coli* BL21 RIL cells (Stratagene). Cells were grown to an A_{595} of 0.6 in LB medium containing ampicillin and chloramphenicol, at which time the expression of $IF3_{mt}$ was induced using 50 μM isopropyl β-D-1-thiogalactopyranoside. Cells were allowed to induce either overnight at 25 °C or for 6 h at 37 °C. After induction, cells were lysed, and $IF3_{mt}$ was purified using Ni-NTA resin followed by S-Sepharose cation exchange chromatography

or HPLC purification using a TSKgel SP-5PW cation exchange column as described previously (*19*). The $IF3_{mt}$ derivatives were tested for structural integrity by comparing the α-helical content obtained using circular dichroism to that of wild-type $IF3_{mt}$ ($IF3_{mt}$:WT). $IF3_{mt}$:1 was excluded from CD measurements because it failed to separate from its truncated 19 kDa fragment during HPLC purification. All mutated proteins exhibited little or no change in α-helical character as compared to the wild-type protein.

Preparation of Polynucleotide Phosphorylase. Initiation complex assays were carried out using poly(A,U,G) as the mRNA. Since this polymer is no longer commercially available, it was prepared using polynucleotide phosphorylase. The gene encoding *E. coli* polynucleotide phosphorylase was previously cloned into the pET11a plasmid in BL21 (DE3) + pLysS cells and was a generous gift from G. H. Jones (Department of Biology, Emory University, Atlanta, GA) (*23*). The enzyme was purified as described previously (*23*). To follow the enzyme during purification, activity assays were carried out. Reaction mixtures (100 μL) contained 50 mM Tris-HCl (pH 8.0), 5 mM $MgCl_2$, 5 mM [^{3}H]ADP (7 cpm/pmol), and 20 μL of appropriate fractions. The reaction mixtures were incubated at 37 °C for 20 min, at which point 500 μg of bovine serum albumin was added and the reaction mixtures were precipitated with cold 5% trichloroacetic acid (*24*). Following final purification of the enzyme, fractions with ADP polymerization activity were pooled and dialyzed against 50% ammonium sulfate overnight without stirring at 4 °C.

Synthesis and Purification of Poly(A,U,G). A 10 mL reaction mixture containing 50 mM Tris-HCl (pH 8.0), 10 mM $MgCl_2$, 5 mM ADP (pH 7.0), 5 mM UDP (pH 7.0), 5 mM GDP (pH 7.0), and 1 mg of polynucleotide phosphorylase was incubated at 37 °C overnight. Following synthesis, the reaction mixture was extracted using phenol (pH 8.0) and chloroform, and the RNA was precipitated with ethanol overnight at −20 °C. RNA was collected by centrifugation at 15000 rpm in the Sorvall SS-34 rotor for 30 min. The pellets were resuspended in 5 mL of sterile H_2O and applied to a Sephadex G-50 column (74 cm × 1.1 cm) equilibrated in 3 mM EDTA (pH 8.0) and 25 mM Tris-HCl (pH 7.8). The column was developed with 150 mL of the same buffer, and 1 mL fractions were collected at a flow rate of 1 mL/min. UV absorbance was monitored at 260 nm. Fractions containing poly(A,U,G) were pooled and precipitated using 2.5 volumes of 100% ethanol overnight at −20 °C. The poly(A,U,G) was collected by centrifugation at 15000 rpm for 30 min in the SS-34 rotor and stored at −20 °C. Before use, the pellets were dissolved in sterile H_2O to a final concentration of 13 μg/μL.

Assay for Initiation Complex Formation on E. coli or Mitochondrial Ribosomes. The effect of $IF3_{mt}$ and its mutated derivatives on the stimulation of [^{35}S]fMet-tRNA binding to either *E. coli* 70S or mitochondrial 55S ribosomes was measured using a filter binding assay and scintillation counting as previously described (*16, 22*). In the assay using *E. coli* ribosomes (100 μL), 2.5−10 pmol of $IF3_{mt}$ (0.025−0.1 μM) was incubated with saturating amounts of $IF2_{mt}$ (16 pmol, 0.16 μM), 70S ribosomes (68 μg, 0.3 μM), poly(A,U,G) (5 μg, 0.05 μg/μL), and [^{35}S]fMet-tRNA (6 pmol, 0.06 μM), under the ionic conditions described previously (*16*). In the assay using mitochondrial 55S ribosomes, 1−4 pmol (0.01−0.04 μM) of $IF3_{mt}$ was incubated with saturating amounts of $IF2_{mt}$ (16 pmol, 0.16 μM), 55S ribosomes (8 pmol, 0.08 μM), poly(A,U,G) (5 μg, 0.05 μg/μL), and [^{35}S]fMet-tRNA (6 pmol, 0.06 μM), under the assay conditions described previously (*16*).

Quantitation of the Binding of $IF3_{mt}$ and Its Derivatives to Mitochondrial 28S Subunits Using Microcon Centrifugation. Ribosome binding reactions were conducted as described previously (*18*). The indicated concentration of $IF3_{mt}$ (0.15−1 pmol, 1.5−10 nM) was incubated with 28S subunits (5 pmol, 50 nM) for 20 min at 25 °C. $IF3_{mt}$ bound to 28S subunits was separated from free $IF3_{mt}$ using a Microcon spin column (Millipore). $IF3_{mt}$ was then released from the ribosome by the addition of EDTA to a final concentration of 20 mM. The amount of $IF3_{mt}$ bound to 28S subunits was determined colorimetrically using a dot blot probed with antibodies against $IF3_{mt}$ as described previously (*18*). A control curve for analysis of the dot blot was prepared by spotting various concentrations of $IF3_{mt}$ (0.5−1.2 pmol, 5−12 nM), 28S (5 pmol, 50 nM), and EDTA (20 mM) directly onto the dot blot nitrocellulose membrane to quantify the change in color versus the amount of protein.

Dissociation of Mitochondrial 55S Ribosomes by $IF3_{mt}$ and Its Mutated Derivatives. Mitochondrial 55S ribosomes (8 pmol, 0.08 μM) were incubated in a buffer containing 50 mM Tris-HCl (pH 7.6), 5 mM $MgCl_2$, 40 mM KCl, and 1 mM dithiothreitol in the absence or presence of 80 pmol (0.8 μM) of $IF3_{mt}$ or its mutated derivatives in a volume of 100 μL at 37 °C for 15 min. The samples were placed on ice for 10 min and then loaded onto a 10 to 30% sucrose gradient and analyzed as previously described by monitoring the A_{254} during fractionation of the gradient (*18*). Each 55S ribosome sample contained some free 39S subunits. Therefore, the percentage of 55S particles was determined by comparing the area of the 55S peak on the absorbance profile to the total area of the 28S, 39S, and 55S peaks combined to account for this contamination. Areas under the peaks were determined using the width of the peak at half the maximal height multiplied by the height. To determine the percentage dissociation, the amount of 55S particles in the absence of $IF3_{mt}$ was set to 100% and compared to the amount of 55S particles observed in the presence of $IF3_{mt}$.

Inhibition of Binding of fMet-tRNA to 28S Subunits by $IF3_{mt}$ in the Absence of mRNA. The inhibition of binding of [^{35}S]fMet-tRNA to 28S subunits in the absence of mRNA was tested as described previously (*16*). Small subunits (6.2 pmol, 0.062 μM) were incubated with saturating amounts of $IF2_{mt}$ (25 pmol, 0.25 μM) and [^{35}S]fMet-tRNA (5 pmol, 0.05 μM) in the presence or absence of $IF3_{mt}$ (0−12 pmol, 0−0.12 μM) or its C-terminal extension-mutated derivatives for 15 min at 25 °C in 100 μL reaction mixtures. The amount of [^{35}S]fMet-tRNA remaining bound to the subunits was determined using a nitrocellulose filter binding assay (*25*).

RESULTS

Design of IF3 Mutations. A model of $IF3_{mt}$ was developed using the modeling program Insight II (Figure 1B). The N-terminal domain was modeled after the crystal structure of *B. stearothermophilus* IF3 [PDB entry 1TIF (*26*)]. This region of IF3 folds into a mixed four-stranded β-sheet packed against a single helical unit (helix 1) lying across the sheet

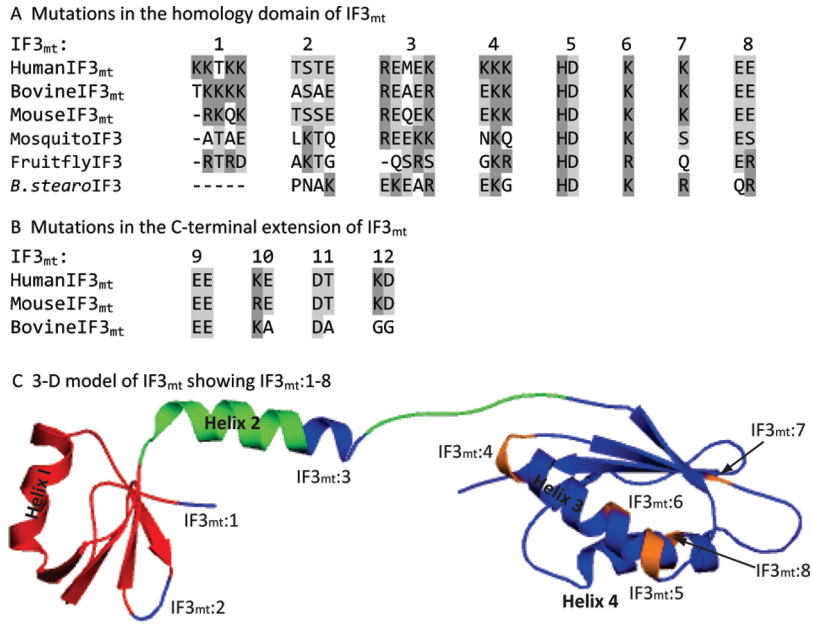

FIGURE 2: Mutations in $IF3_{mt}$. (A) Conservation of the charged residues mutated in $IF3_{mt}$:1−8. Positively charged residues are highlighted in dark gray, and negatively charged residues are highlighted in light gray. The numbers above each cluster of residues indicate the $IF3_{mt}$ derivative containing mutations of those residues. *B. stearothermophilus* IF3 does not have residues corresponding to $IF3_{mt}$:1. These residues are present in *E. coli* IF3 as KRVQT. (B) Sequence conservation of $IF3_{mt}$:9−12 among the vertebrate lineage. Positively charged residues are highlighted in dark gray, and negatively charged residues are highlighted in light gray. (C) Model of $IF3_{mt}$ showing $IF3_{mt}$:1−8. The N-terminal domain is colored red and the linker green, and the mutated residues are colored blue. $IF3_{mt}$:1 could not be modeled on the basis of the crystal structure of *B. stearothermophilus* because these residues are not present in this IF3 or in the NMR structure of the N-domain of *E. coli* IF3 (*38*). $IF3_{mt}$:1 has been placed in the model at the N-terminus of the protein for illustrative purposes. The C-terminal homology domain is colored blue, and the mutated residues are colored orange.

and a second α-helix (helix 2) extending into the linker region. The model of the N-terminus of $IF3_{mt}$ is quite similar to that of the crystal structure of the *B. stearothermophilus* factor despite the low percent identity (<23%) between the N-terminal domains. The C-terminal domain was modeled after the NMR structure of mouse $IF3_{mt}$ [PDB entry 2CRQ (manuscript to be published)] which has been shown to consist of two α-helices (H3 and H4) lying on top of a four-stranded β-sheet. The sequence of the C-terminal domain of the human factor is 72% identical to that of mouse $IF3_{mt}$. The predicted structure of this domain of human $IF3_{mt}$ is quite similar to that of the mouse factor except that one of the β-strands is modeled in two sections due to the presence of an internal proline residue. In the model, the linker region is depicted as being partially α-helical. However, biochemical studies of the linker regions of IF3 from several sources suggest that this region has considerable flexibility (*17, 27*−*29*). The model does not include the N- and C-terminal extensions, which were predicted to be disordered. In the current work, a number of residues in $IF3_{mt}$, predicted to lie on the surface of the protein, were mutated, and the effects of these mutations on the ability of $IF3_{mt}$ to promote initiation complex formation and to bind to 28S subunits were examined.

Mitochondrial 55S ribosomes are composed of approximately two-thirds protein and one-third RNA. The interface between the 28S and 39S subunits is rich in RNA (*3*). Significant electrostatic interactions between $IF3_{mt}$ (pI ∼10) and the 12S small subunit rRNA are expected to play an important role in the function of this factor. To identify residues in $IF3_{mt}$ potentially involved in binding to the small subunit or in other functions of this factor, clusters of charged amino acids predicted to be exposed on the surface in the model of $IF3_{mt}$ (Figure 1B) were changed to alanine (Figure 2). Twelve different mutated derivatives ($IF3_{mt}$:1−12) were made in the N- and C-terminal domains, the linker, and the C-terminal extension. The charges of these residues are generally conserved among vertebrate $IF3_{mt}$, and partially conserved with the mosquito, fruit fly, and bacterial factors (Figure 2A). No mutations were made in the N-terminal extension, because this region is poorly conserved and no known function has been attributed to the N-terminal extension alone.

The N-terminal domain of *E. coli* IF3 does not bind independently to 30S subunits (*12*). In contrast, the N-terminal domain of $IF3_{mt}$ binds 28S subunits with a K_d of 390 ± 60 nM (*17*). Two clusters of residues in the N-terminal domain were mutated (Figure 2). The selected residues were fairly well conserved among the mammalian factors (Figure 2A) but less conserved with the $IF3_{mt}$ of other organisms. $IF3_{mt}$:1 is located five residues into the N-terminal domain of $IF3_{mt}$ in a region where no structural information is available. Its predicted location is shown in the model (Figure 2C). This region was selected for mutagenesis since the first six residues of *E. coli* IF3 are important for the function of this factor (*30*). $IF3_{mt}$:2 is also located in the N-terminal domain in a loop between two β-strands facing away from the linker region. $IF3_{mt}$:3 is located in a predicted α-helical region in the $IF3_{mt}$ linker. $IF3_{mt}$:4−6 are located in the C-terminal domain of $IF3_{mt}$ in an α-helix (helix 3) predicted previously to be essential for the function of the *E. coli* protein (*31*). $IF3_{mt}$:7 is also in the C-terminal domain at the tip of a β-strand (corresponding to β-strand 7 in the prokaryotic factors) in the center of the domain. $IF3_{mt}$:8 is located behind $IF3_{mt}$:7 on the opposite face of the C-terminal domain (Figure 2C). $IF3_{mt}$:9−12 are located in the C-terminal

extension of $IF3_{mt}$, where no structural data are currently available. A summary of the $IF3_{mt}$ mutations is given in Table 1.

The mutated proteins were purified and tested for structural integrity by measuring the α-helical content using circular dichroism. The activities of the derivatives in promoting binding of fMet-tRNA to *E. coli* and mitochondrial ribosomes were tested. Proteins that exhibited reduced activity in promoting initiation complex formation were further tested for their abilities to dissociate mitochondrial 55S ribosomes. Those unable to dissociate 55S ribosomes were tested for their abilities to bind to mitochondrial 28S small subunits.

Mutations in the N-Terminal Domain and Linker. $IF3_{mt}$ derivatives with mutations in the N-terminal domain and linker were tested for their abilities to promote binding of fMet-tRNA to both *E. coli* and mitochondrial ribosomes in the presence of $IF2_{mt}$. This assay primarily measures the ribosomal subunit dissociation activity of this factor (*22*). A representative graph showing initiation complex formation as a function of increasing amounts $IF3_{mt}$ is shown in Figure 3A. $IF3_{mt}$:1 and $IF3_{mt}$:2 showed activity similar to that of the unmutated factor ($IF3_{mt}$:WT) on both *E. coli* and mitochondrial ribosomes (Figure 3B), indicating that these residues are not important for the activity of this protein. $IF3_{mt}$:3, located in the linker region of the protein, showed a slight reduction in activity in initiation complex formation on both *E. coli* and mitochondrial ribosomes (Figure 3B). The slight loss of activity for $IF3_{mt}$:3 was further explored in an assay that measures the ability of the protein to dissociate mitochondrial 55S ribosomes as described below. $IF3_{mt}$:3 showed the same subunit dissociation pattern as the wild-type protein in this assay, which indicates that it did not have any significant defect in this function (Figure 4D).

Mutations in the C-Terminal Domain. The C-terminal domain of $IF3_{mt}$ with the linker binds to the small ribosomal subunit with nearly the same affinity as the full-length protein and shows the same activity as the full-length protein in stimulating binding of fMet-tRNA to mitochondrial ribosomes (*17*). $IF3_{mt}$ derivatives with mutations in the C-terminal domain were tested for activity in initiation complex formation on *E. coli* and mitochondrial ribosomes. $IF3_{mt}$:7 and $IF3_{mt}$:8 had the same activity as the wild-type protein (Figure 3). $IF3_{mt}$:4 exhibited slightly reduced activity but still maintained its ability to dissociate 55S ribosomes as well as the wild-type protein (Figure 4). However, $IF3_{mt}$:5 and $IF3_{mt}$:6 had almost no activity in promoting initiation complex formation on *E. coli* ribosomes and had significantly reduced activity on mitochondrial ribosomes (Figure 3).

Since neither $IF3_{mt}$:5 nor $IF3_{mt}$:6 was active in stimulating initiation complex formation, an assay that basically measures ribosome dissociation, their abilities to promote the dissociation of 55S ribosomes were examined directly by sucrose density centrifugation. Both proteins were deficient in dissociation activity [$IF3_{mt}$:6 (Figure 4) and $IF3_{mt}$:5 (data not shown)]. $IF3_{mt}$:5 dissociated 55S ribosomes by only ~15%, compared to just more than 50% dissociation with the same level of $IF3_{mt}$:WT. $IF3_{mt}$:6 had essentially no activity in the ribosome dissociation assay.

One possible explanation for the lack of activity observed with $IF3_{mt}$:5 and $IF3_{mt}$:6 is that these mutated proteins are unable to bind 28S subunits and, therefore, are unable to effectively prevent the interaction of the 28S and 39S ribosomal subunits. To test this possible explanation directly, the binding of $IF3_{mt}$ and its mutated derivatives to 28S subunits was assessed using Microcon-100 centrifugation followed by immunological detection of $IF3_{mt}$ on a dot blot apparatus (*18*). This method takes advantage of the observation that, in the absence of 28S subunits, $IF3_{mt}$ passes through the membrane while $IF3_{mt}$ bound to 28S subunits does not. $IF3_{mt}$:WT binds to 28S subunits with a K_d of 35 ± 13 nM (Table 3). As indicated in Figure 5, $IF3_{mt}$:6 binds 28S subunits with a K_d of 45 ± 17 nM and $IF3_{mt}$:5 binds to 28S subunits with a K_d of 19 ± 11 nM. Since both mutated proteins exhibit the same binding to 28S subunits as $IF3_{mt}$:WT, the lack of activity of the mutated proteins in initiation complex formation and in the dissociation of 55S ribosomes into the 28S and 39S subunits cannot be attributed to a defect in their abilities to bind the small ribosomal subunit.

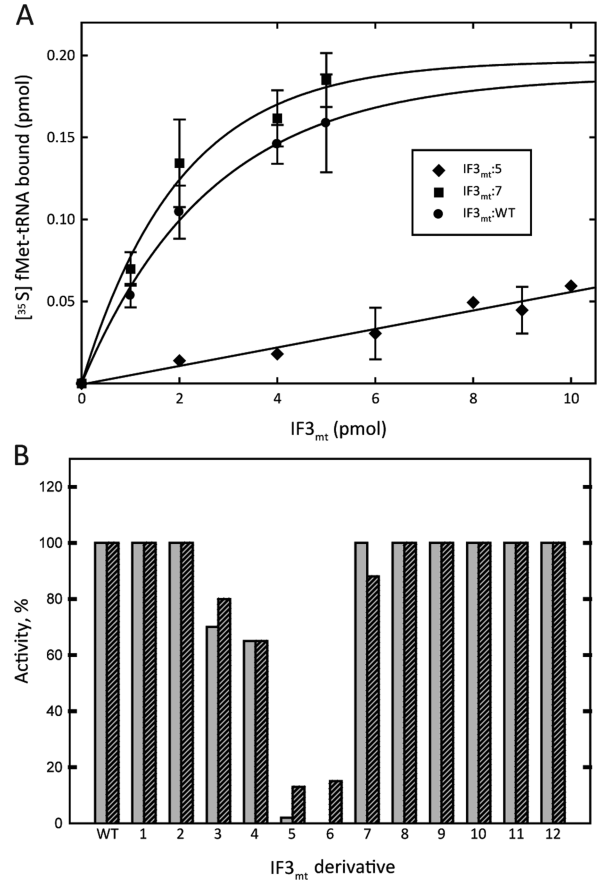

FIGURE 3: Effect of mutated derivatives of $IF3_{mt}$ on initiation complex formation. (A) Effect of $IF3_{mt}$:WT, $IF3_{mt}$:7, and $IF3_{mt}$:5 on initiation complex formation on mitochondrial 55S ribosomes. Binding of [^{35}S]fMet-tRNA to mitochondrial 55S particles was tested in the presence of saturating amounts of $IF2_{mt}$ using $IF3_{mt}$:WT (●), $IF3_{mt}$:7 (■), or $IF3_{mt}$:5 (◆). A blank representing the amount of [^{35}S]fMet-tRNA bound to ribosomes in the absence of $IF3_{mt}$ (~0.1 pmol) was subtracted from each value. (B) Summary of the activities of $IF3_{mt}$:1−12 in initiation complex formation. This assay primarily measures ribosome dissociation. The activity of $IF3_{mt}$:WT was set to 100%, and the values of the mutated derivatives were compared to that value using the linear regions of the dose−response curves. The activities on 70S ribosomes are shown with gray bars, while activities on mitochondrial ribosomes are shown with striped gray bars. Derivatives identical to the wild type within error are shown as 100%.

Mutations in the C-Terminal Extension. One unusual property of $IF3_{mt}$ is that its C-terminal extension is thought to play an important role in decreasing the amount of fMet-

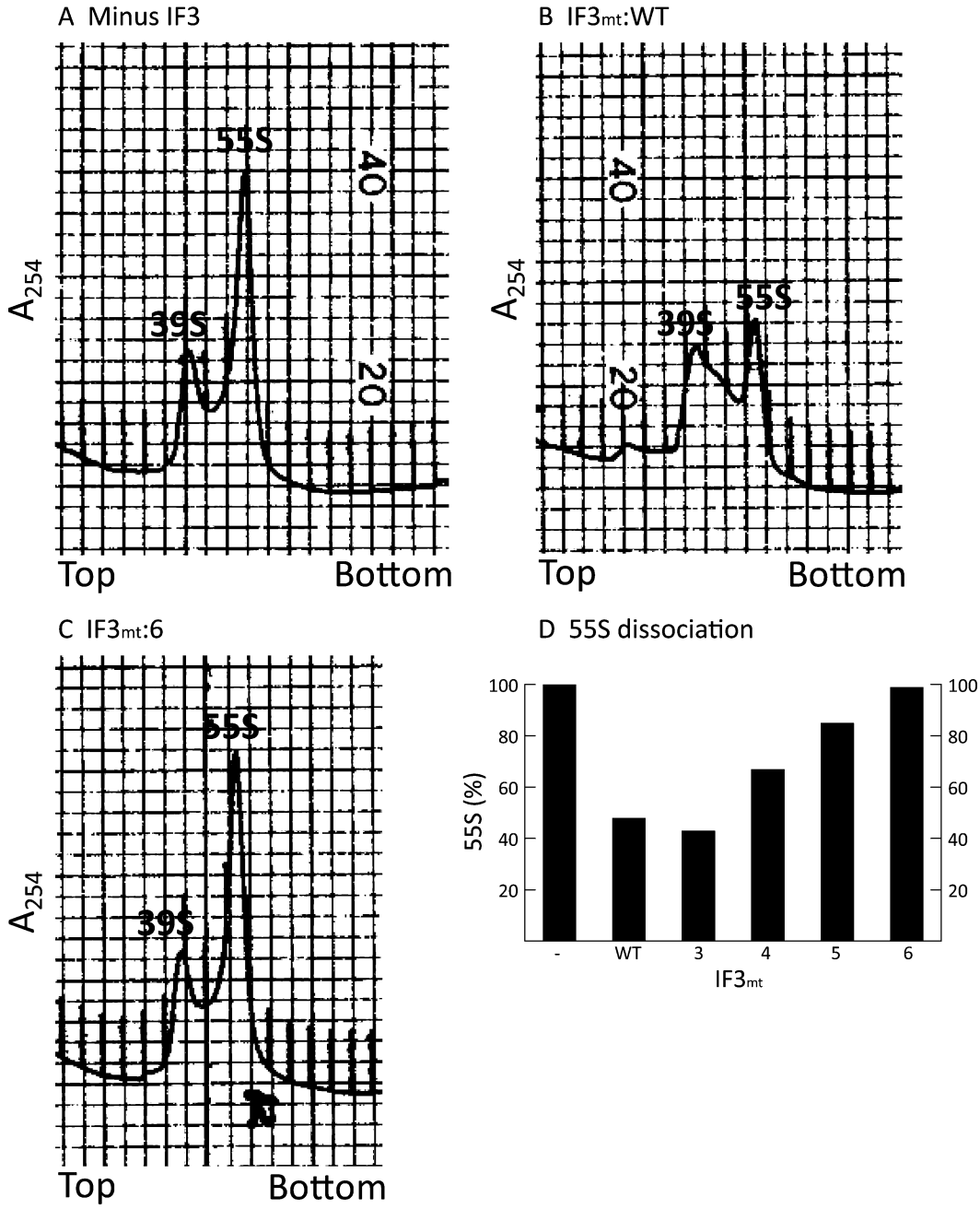

FIGURE 4: Effect of $IF3_{mt}$ and its mutated derivates on the dissociation of mitochondrial 55S ribosomes. Fractionation profiles of mitochondrial 55S ribosomes after centrifugation on a 10 to 30% sucrose gradient. Mitochondrial 55S ribosomes (8 pmol) were incubated as described in Materials and Methods in the absence (A) or presence of 80 pmol of $IF3_{mt}$ (B) or its mutated derivative $IF3_{mt}$:6 (C) and subsequently subjected to centrifugation on a 10 to 30% sucrose density gradient. Gradients were fractionated while the A_{254} was monitored. (D) Percentage of mitochondrial 55S ribosomes remaining after the addition of $IF3_{mt}$:WT or its mutated derivatives as measured by sucrose density gradient centrifugation.

Table 3: Binding of $IF3_{mt}$ and Its Mutated Derivatives to 28S Mitochondrial Subunits[a]

$IF3_{mt}$	K_d (nM)
$IF3_{mt}$:WT	35 ± 13
$IF3_{mt}$:5	19 ± 11
$IF3_{mt}$:6	45 ± 17

[a] K_d values of $IF3_{mt}$:WT and its mutated derivatives binding to 28S mitochondrial subunits as determined by Microcon centrifugation.

tRNA bound to mitochondrial 28S subunits in the absence of mRNA. This observation suggests that mRNA binding should precede fMet-tRNA binding in the mitochondrial system (*16*). No structural data are currently available for the C-terminal extension of $IF3_{mt}$. Modeling of this region indicated that it is probably disordered in solution. Regions of highly charged amino acids (acidic and basic) conserved in vertebrate $IF3_{mt}$ lineages were selected for mutation to alanine residues (Figure 2). All of these derivatives were as active as $IF3_{mt}$:WT in promoting initiation complex formation on both *E. coli* and mitochondrial ribosomes (Figure 3). As indicated in Figure 6, $IF3_{mt}$:WT inhibits the binding of fMet-tRNA to 28S subunits in the absence of mRNA. $IF3_{mt}$:5 and $IF3_{mt}$:6 in the C-terminal domain, along with $IF3_{mt}$:10, $IF3_{mt}$:11, and $IF3_{mt}$:12 in the C-terminal extension, exhibited normal activity in this assay (data not shown). However, $IF3_{mt}$:9, also in the C-terminal extension, was unable to reduce the amount of fMet-tRNA bound to ribosomes in the

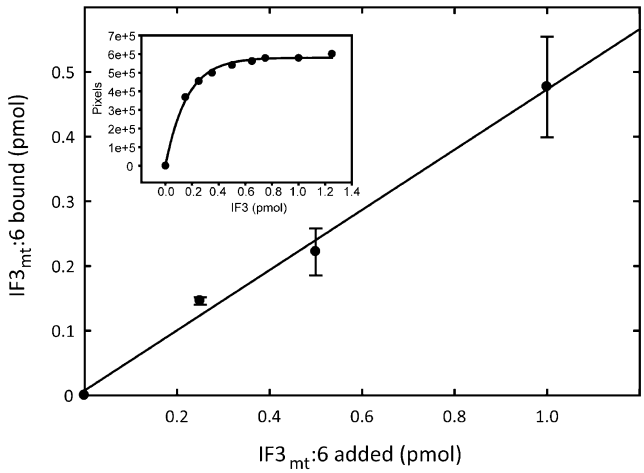

FIGURE 5: Binding of $IF3_{mt}$:6 to 28S subunits. Binding assays were performed using a Microcon spin column as described previously (*18*). The inset shows a calibration curve of $IF3_{mt}$:WT using a colorimetric assay and a dot blot apparatus. This curve was used to determine the amount of $IF3_{mt}$ bound to mitochondrial 28S ribosomes in the Microcon centrifugation assay as described in Materials and Methods.

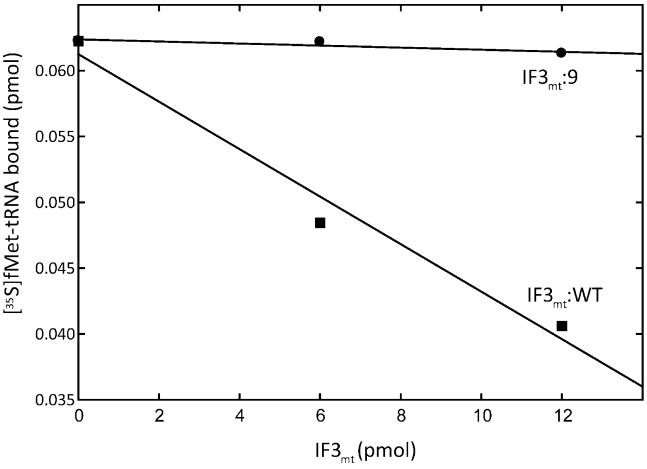

FIGURE 6: $IF3_{mt}$-mediated inhibition of binding of fMet-tRNA to mitochondrial 28S subunits in the absence of mRNA. Mitochondrial 28S subunits were incubated with saturating amounts of $IF2_{mt}$ and [^{35}S]fMet-tRNA in the presence or absence of $IF3_{mt}$:WT or its C-terminal extension-mutated derivative $IF3_{mt}$:9 as described previously (*16*). The amount of [^{35}S]fMet-tRNA remaining bound to the filter in the presence of $IF3_{mt}$:WT (■) or $IF3_{mt}$:9 (●) was determined using a nitrocellulose filter binding assay.

absence of mRNA (Figure 6). This observation pinpoints a region of the C-terminal extension that is critical for inhibiting initiation complex formation before the mRNA is bound. Interestingly, the linker region of $IF3_{mt}$ also appears to have a role in preventing fMet-tRNA binding in the absence of mRNA (*17*).

The C-terminal extension is predicted to emerge from the C-terminal domain near the linker region according to the model (Figure 1B). The linker, and, thus, the C-terminal extension, may span the region between the platform, where the C-terminal domain is thought to bind, and the head of the small subunit. The linker may be positioned toward the mRNA binding channel as predicted in the model of McCutcheon et al. (*13*). A transient association between these regions of $IF3_{mt}$ and the mRNA channel near the P-site may permit this factor to distinguish prematurely formed initiation complexes.

DISCUSSION

Comparison of Mutational Effects in $IF3_{mt}$ and E. coli IF3. Both NMR (*32*) and mutational analysis (*31, 33*) indicate that there are a number of contacts between *E. coli* IF3 and the small subunit in the C-terminal domain. These interactions appear to span much of helix 3, the loop regions, and portions of helix 4. Key differences between $IF3_{mt}$ and the *E. coli* factor become apparent when the extensive battery of mutations made to Arg residues in *E. coli* IF3 are compared to those presented here in the mitochondrial factor (Figure 7). In *E. coli* IF3, the most drastic effects on the activity of the factor in initiation complex formation measured by ribosomal subunit dissociation were caused by a mutation in the center of helix 4 in the C-terminal domain (*31*). This mutation also caused significant reductions in the level of binding of the mutated protein to *E. coli* 30S ribosomal subunits, suggesting that the defect in initiation arises from a weaker interaction with the small subunit. However, $IF3_{mt}$:8, located in helix 4 in the C-terminal domain of $IF3_{mt}$, was able to stimulate initiation complex formation as well as the wild-type factor. This observation suggests that residues in helix 4 may play a less important role in $IF3_{mt}$ than in *E. coli* IF3.

In the mitochondrial factor, the most drastic effects were seen with two mutations in helix 3 [$IF3_{mt}$:5 and $IF3_{mt}$:6 (Figure 7)]. A mutation made in the center of this helix in *E. coli* IF3 (R112S) had an only modest effect on initiation complex formation (*31*), and the mutated derivative still retained >60% of the activity observed with the wild-type factor. In the mitochondrial factor, the mutations in helix 3 are located closer to the base of the helix rather than in the center. The side chains of these residues are predicted to be shifted approximately 90° toward the front of the protein when compared to the side chain of the mutated residues in *E. coli* IF3. $IF3_{mt}$ derivatives containing these mutations do not promote initiation complex formation but are still able to bind to mitochondrial 28S subunits. Thus, residues near the bottom of helix 3 are not predicted to be in direct contact with the 28S subunits. Rather, they may define a surface of $IF3_{mt}$ that contacts the 39S subunit during the dissociation of the 55S ribosomes into subunits.

Model for $IF3_{mt}$-Mediated Dissociation of 55S Ribosomes. Mutation of residues 170−171, and 175 in helix 3 of the C-terminal domain of $IF3_{mt}$ drastically reduced the activity of $IF3_{mt}$ in promoting initiation complex formation. This assay basically measures the ability of $IF3_{mt}$ to dissociate 55S ribosomes. Sucrose density gradient centrifugation confirmed the idea that these mutations inactivate $IF3_{mt}$ in ribosomal subunit dissociation. The most logical explanation for these results is that the mutated proteins fail to bind mitochondrial 28S subunits and, therefore, cannot prevent 39S joining. However, both of these mutated derivatives of $IF3_{mt}$ bind to 28S subunits as well as the wild-type factor (Table 3). This observation indicates that an alternative problem must underlie the loss of activity in these mutated $IF3_{mt}$ derivatives. One possible explanation is that there are two distinct functionally important surfaces of $IF3_{mt}$. The first surface would function as a dissociation interface and may interact with one or both of the ribosomal subunits. The second surface would function as a binding interface between the factor and the 28S subunit.

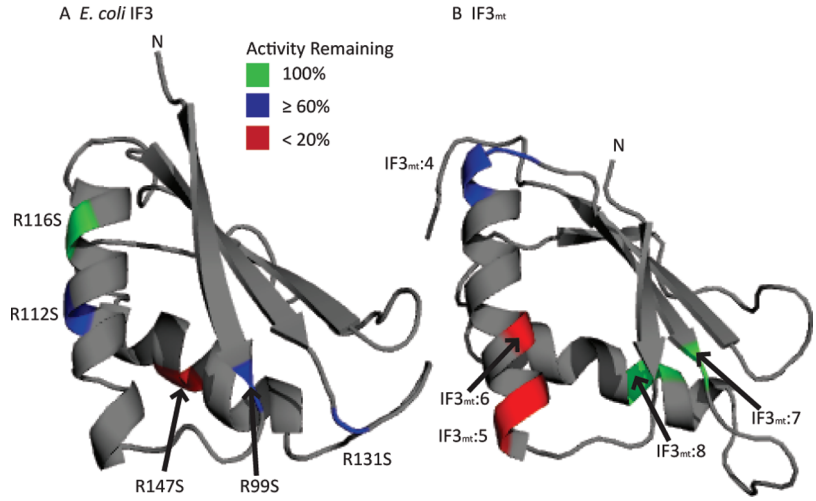

FIGURE 7: Effects of mutations in the C-terminal domain of *E. coli* IF3 and $IF3_{mt}$. (A) Mutated residues in the C-terminal domain of *E. coli* IF3 and their effects on activity in initiation complex formation on *E. coli* ribosomes. The activity remaining was based on 70S dissociation, one of several assays carried out with these mutated derivatives of *E. coli* IF3. The most drastic effects on activity are seen with the mutation in the center of the α-helix (helix 4) on the back of the protein. (B) Mutated residues in the C-terminal domain of $IF3_{mt}$ and the effects of these mutations on activity in initiation complex formation on mitochondrial ribosomes. The most drastic effects are seen with the two mutations located at the base of helix 3.

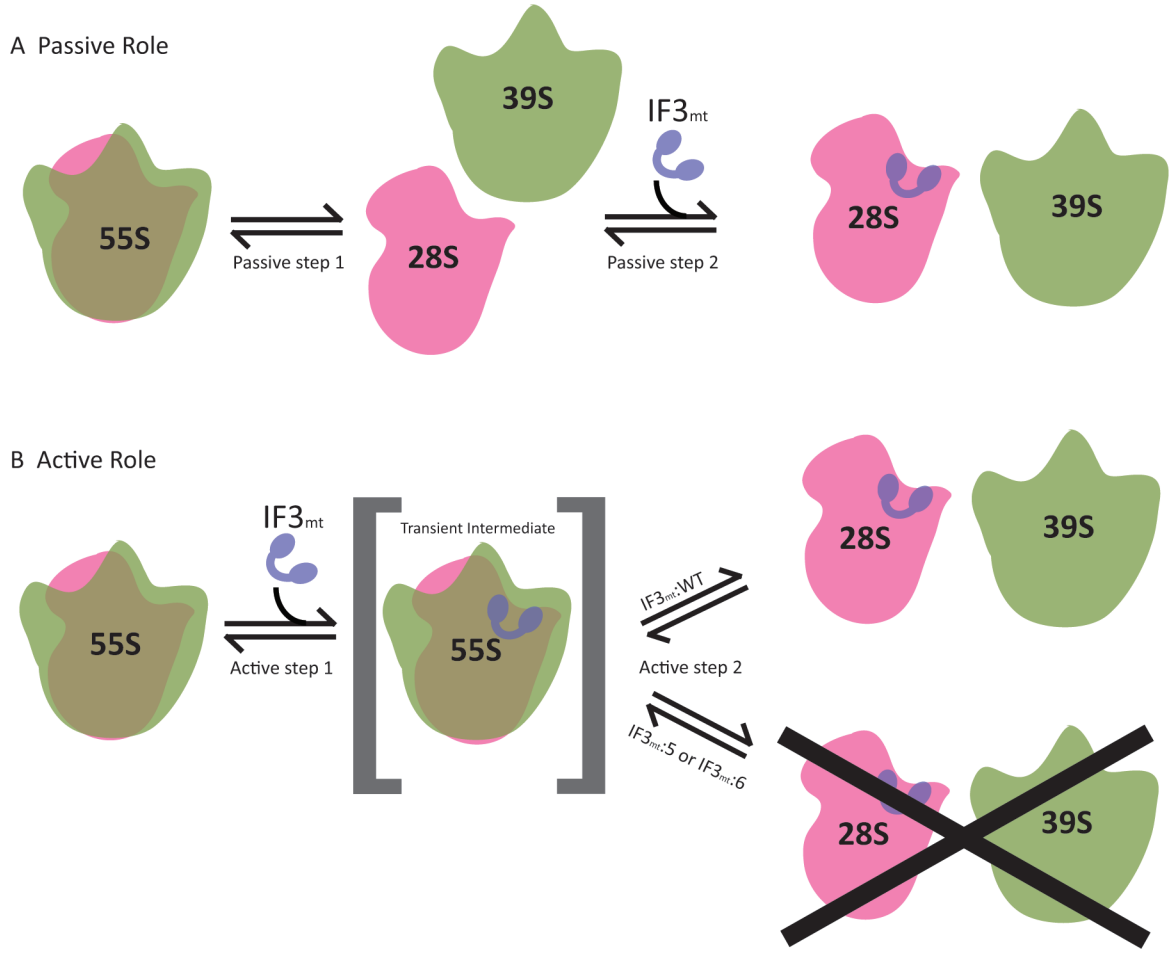

FIGURE 8: Models for the mechanism of $IF3_{mt}$ in the dissociation of mitochondrial ribosomes. (A) In the passive model, the subunits are in equilibrium with the 55S monosome (passive step 1). $IF3_{mt}$ binds to free 28S subunits, preventing reassociation with the 39S subunit (passive step 2). (B) In the active model, $IF3_{mt}$ interacts with the 55S particle, forming a transient 28S−$IF3_{mt}$−39S complex (active step 1), which then dissociates into a 28S−$IF3_{mt}$ complex and free 39S subunits (active step 2).

Recent work has indicated that the position of the C-terminal domain of *E. coli* IF3 blocks bridge B2b of the 70S ribosome, preventing the association of the large and small subunits when IF3 is present (*14*). Bridge B2b involves 16S rRNA nucleotide 794 (*34*), which is in the proximity of the proposed IF3 binding site on the 30S subunit (*8, 35*). Cryo-electron microscopy studies of mammalian mitochondrial ribosomes (*3*) indicate that this

intersubunit bridge is one of several conserved contacts between the two subunits. $IF3_{mt}$ is expected to bind to 28S subunits in a manner similar to the binding of *E. coli* IF3 to 30S subunits. It is likely that residues 170−171, and 175 play an essential role in allowing $IF3_{mt}$ to block the formation of bridge B2b. Mutation of these residues could impede the blocking of this intersubunit bridge by $IF3_{mt}$, preventing these mutated forms of $IF3_{mt}$ from effectively competing with the 39S subunit for binding to the 28S subunit.

There are two current models to explain the action of $IF3_{mt}$ in ribosomal subunit dissociation (Figure 8). In the passive model, $IF3_{mt}$ binds to 28S subunits after the subunits dissociate transiently (Figure 8A, passive model). In this model, $IF3_{mt}$ acts more as an anti-association factor than a dissociation factor (*36*). In the active model, an equilibrium exists between 55S ribosomes and a transient 28S−IF3−39S complex (Figure 8B, active step 1). This transient complex is in equilibrium with free 39S subunits and 28S subunits bound to $IF3_{mt}$ (active step 2). The active model suggests that $IF3_{mt}$ plays a more direct role in dissociating 55S ribosomes than simply binding to 28S subunits that are present at equilibrium. $IF3_{mt}$:5 and $IF3_{mt}$:6, though they bind well to 28S subunits (active step 1), are deficient in dissociating 55S ribosomes (active step 2). This observation suggests that a transient 28S−IF3−39S complex formed by these mutated derivatives fails to dissociate into its component subunits. This idea is supposed by recent kinetic data, which suggest that in *E. coli*, IF3 may remain associated with the 30S subunit that is partially bound to the 50S subunit (*14*), and by recent cryo-electron microscopy data, which tentatively suggest that IF3 may not be released from 70S particles until the hydrolysis of GTP by IF2 has occurred (*37*). These results suggest that $IF3_{mt}$ plays an active role rather than a passive role in ribosomal subunit dissociation in the mitochondrial translational system.

ACKNOWLEDGMENT

We thank Brenda Temple (University of North Carolina) for help with the molecular modeling. We thank Emdadul Haque and Christie Jones (University of North Carolina) for helpful discussions.

REFERENCES

1. Lin, M. T., and Beal, M. F. (2006) Mitochondrial dysfunction and oxidative stress in neurodegenerative diseases. *Nature 443*, 787–795.
2. Scheffler, I. (1999) *Mitochondria*, Wiley-Liss, Inc., New York.
3. Sharma, M. R., Koc, E. C., Datta, P. P., Booth, T. M., Spremulli, L. L., and Agrawal, R. K. (2003) Structure of the mammalian mitochondrial ribosome reveals an expanded functional role for its component proteins. *Cell 115*, 97–108.
4. Gualerzi, C., and Pon, C. (1990) Initiation of mRNA translation in prokaryotes. *Biochemistry 29*, 5881–5889.
5. Cummings, H., and Hershey, J. (1994) Translation initiation factor IF-1 is essential for cell viability in *Escherichia coli*. *J. Bacteriol. 176*, 198–205.
6. Gaur, R., Grasso, D., Datta, P. P., Krishna, P. D. V., Das, G., Spencer, A., Agrawal, R. K., Spremulli, L., and Varshney, U. (2008) A single mammalian mitochondrial translation initiation factor functionally replaces two bacterial factors. *Mol. Cell 29*, 180–190.
7. Dottavio-Martin, D., Suttle, D. P., and Ravel, J. M. (1979) The effects of initiation factors IF-1 and IF-3 on the dissociation of *Escherichia coli* 70 S ribosomes. *FEBS Lett. 97*, 105–110.
8. Dallas, A., and Noller, H. F. (2001) Interaction of translation initiation factor 3 with the 30S ribosomal subunit. *Mol. Cell 8*, 855–864.
9. Paci, M., Pon, C., Lammi, M., and Gualerzi, C. (1984) Structure-function relationship in *Escherichia coli* translational initiation factors. Characterization of IF-3 by high resolution ^{1}H NMR spectroscopy. *J. Biol. Chem. 259*, 9628–9634.
10. La Teana, A., Gualerzi, C., and Brimacombe, R. (1995) From stand-by to decoding site. Adjustment of the mRNA on the 30S subunit under the influence of the initiation factors. *RNA 1*, 772–782.
11. Antoun, A., Pavlov, M. Y., Lovmar, M., and Ehrenberg, M. (2006) How initiation factors tune the rate of initiation of protein synthesis in bacteria. *EMBO J. 25*, 2539–2550.
12. Petrelli, D., LaTeana, A., Garofalo, C., Spurio, R., Pon, C. L., and Gualerzi, C. O. (2001) Translation initiation factor IF3: Two domains, five functions, one mechanism? *EMBO J. 20*, 4560–4569.
13. McCutcheon, J., Agrawal, R., Philips, S. M., Grassucci, R., Gerchman, S., Clemons, W. M., Ramakrishnan, V., and Frank, J. (1999) Location of translational initiation factor IF3 on the small ribosomal subunit. *Proc. Natl. Acad. Sci. U.S.A. 96*, 4301–4306.
14. Fabbretti, A., Pon, C. L., Hennelly, S. P., Hill, W., Lodmell, J., and Gualerzi, C. O. (2007) The real-time path of translation factor IF3 onto and off the ribosome. *Mol. Cell 25*, 285–296.
15. Laursen, B. S., Sorensen, H. P., Mortensen, K. K., and Sperling-Petersen, H. U. (2005) Initiation of protein synthesis in bacteria. *Microbiol. Mol. Biol. Rev. 69*, 101–123.
16. Bhargava, K., and Spremulli, L. L. (2005) Role of the N- and C-terminal extensions on the activity of mammalian mitochondrial translational initiation factor 3. *Nucleic Acids Res. 33*, 7011–7018.
17. Haque, M., and Spremulli, L. L. (2008) Roles of the N- and C-terminal domains of mammalian mitochondrial initiation factor 3 in protein biosynthesis. *J. Mol. Biol. 384*, 929–940.
18. Haque, M. E., Grasso, D., and Spremulli, L. L. (2008) The interaction of mammalian mitochondrial translational initiation factor 3 with ribosomes: Evolution of terminal extensions in $IF3_{mt}$. *Nucleic Acids Res. 36*, 589–597.
19. Grasso, D. G., Christian, B. E., Spencer, A. C., and Spremulli, L. L. (2007) Over-expression and purification of mitochondrial translational initiation factor 2 and initiation factor 3. *Methods Enzymol., 430,* 59–78.
20. Spremulli, L. L. (2007) *Methods in Molecular Biology*, Vol 372; Mitochondria, Practical Protocols (Leister, D., and Herrmann, J., Eds.) pp 265−275, Humana Press, Totowa, NJ.
21. Graves, M., and Spremulli, L. L. (1983) Activity of *Euglena gracilis* chloroplast ribosomes with prokaryotic and eukaryotic initiation factors. *Arch. Biochem. Biophys. 222*, 192–199.
22. Koc, E. C., and Spremulli, L. L. (2002) Identification of mammalian mitochondrial translational initiation factor 3 and examination of its role in initiation complex formation with natural mRNAs. *J. Biol. Chem. 277*, 35541–35549.
23. Jones, G. H., Symmons, M. F., Hankins, J. S., and Mackie, G. A. (2003) Overexpression and purification of untagged polynucleotide phosphorylases. *Protein Expression Purif. 32*, 202–209.
24. Spencer, A. C., Heck, A. H., Takeuchi, N., Watanabe, K., and Spremulli, L. L. (2004) Characterization of the human mitochondrial methionyl-tRNA synthetase. *Biochemistry 43*, 9743–9754.
25. Liao, H.-X., and Spremulli, L. L. (1991) Initiation of protein synthesis in animal mitochondria: Purification and characterization of translational initiation factor 2. *J. Biol. Chem. 266*, 20714–20719.
26. Biou, V., Shu, F., and Ramakrishnan, V. (1995) X-ray crystallography shows that translational initiation factor IF3 consists of two compact α/β domains linked by an α-helix. *EMBO J. 14*, 4056–4064.
27. Moreau, M., de Cock, E., Fortier, P.-L., Garcia, C., Albaret, C., Blanquet, S., Lallemand, J.-Y., and Dardel, F. (1997) Heteronuclear NMR studies of *E. coli* translation initiation factor IF3. Evidence that the inter-domain region is disordered in solution. *J. Mol. Biol. 266*, 15–22.
28. Hua, Y., and Raleigh, D. (1998) On the global architecture of initiation factor IF3: A comparative study of the linker regions from the *Escherichia coli* protein and the *Bacillus stearothermophilus* protein. *J. Mol. Biol. 278*, 871–878.

29. de Cock, E., Springer, M., and Dardel, F. (1999) The interdomain linker of *Escherichia coli* initiation factor IF3: A possible trigger of translation initiation specificity. *Mol. Microbiol. 32*, 193–202.
30. Lammi, M., Pon, C., and Gualerzi, C. (1987) The NH_2-terminal cleavage of *Escherichia coli* translational initiation factor 3: A mechanism to control the intracelllular level of the factor. *FEBS Lett. 215*, 115–121.
31. Petrelli, D., Garofalo, C., Lammi, M., Spurio, R., Pon, C. L., Gualerzi, C. O., and Teana, A. L. (2003) Mapping the active sites of bacterial translation initiation factor IF3. *J. Mol. Biol. 331*, 541–556.
32. Sette, M., Spurio, R., VanTilborg, P., Gualerzi, C., and Boelens, R. (1999) Identification of the ribosome binding sites of translation initiation factor IF3 by multidimensional heteronuclear NMR spectroscopy. *RNA 5*, 82–92.
33. Bellis, D., Liveris, D., Goss, D., Ringquist, S., and Schwartz, I. (1992) Structure-function analysis of *Escherichia coli* translation initiation factor 3: Tyrosine 107 and lysine 110 are required for ribosome binding. *Biochemistry 31*, 11984–11990.
34. Liiv, A., and O'Connor, M. (2006) Mutations in the intersubunit bridge regions of 23S rRNA. *J. Biol. Chem. 281*, 29850−29862.
35. Tapprich, W., Goss, D., and Dahlberg, A. (1989) Mutation at position 791 in *Escherichia coli* 16 S ribosomal RNA affects processes involved in the initiation of protein synthesis. *Proc. Natl. Acad. Sci. U.S.A. 86*, 4927–4931.
36. Naaktgeboren, N., Roobol, K., and Voorma, H. O. (1977) The effect of initiation factor IF-1 on the dissociation of 70S ribosomes of *Escherichia coli*. *Eur. J. Biochem. 72*, 49–56.
37. Allen, G. S., Zavialov, A., Gursky, R., Ehrenberg, M., and Frank, J. (2005) The cryo-EM structure of a translation initiation complex from *Escherichia coli*. *Cell 121*, 703–712.
38. Garcia, C., Fortier, P.-L., Blanquet, S., Lallemand, J.-Y., and Dardel, F. (1995) ^{1}H and ^{15}N resonance assignments and structure of the N-terminal domain of *Escherichia coli* initiation factor 3. *Eur. J. Biochem. 228*, 395–402.

BI8023493